

Application of fractional calculus to viscoelastic behaviour modelling and to the physical ageing phenomenon in glassy amorphous polymers

M. Alcoutlabi* and J. J. Martinez-Vega

Laboratoire Matériaux Polymères et Composites, Université de Savoie, Campus Scientifique, 73376 Le Bourget du Lac Cedex, France

(Received 13 October 1997; accepted 19 January 1998)

A model based on the concept of fractional calculus is proposed to predict the viscoelastic behaviour of amorphous polymers in the temperature range from $T_g - 190^\circ\text{C}$ to $T_g + 25^\circ\text{C}$. Poly methyl methacrylate (PMMA) has been chosen as a model amorphous polymer. PMMA has been studied by dynamic mechanical spectrometry and the experimental data have been compared with the fractional calculus model proposed. An agreement between experiments and model has been achieved. PMMA is characterised by an unstable non-equilibrium state, at least between the main secondary relaxation (β) and the main relaxation (α). All molecular mobility phenomena are affected by this structural recovery that itself exists because of molecular mobility. One of the objectives of this work is to give some ideas of this important phenomenon and quantify its influence on the parameters of the viscoelastic model proposed. © 1998 Elsevier Science Ltd. All rights reserved.

(Keywords: fractional calculus; poly(methyl methacrylate); physical ageing)

INTRODUCTION

The simplest way to characterise the mechanical properties of a polymer is to measure its elastic modulus as a function of temperature. But, since polymers are viscoelastic materials, their modulus depends on time and method of measurement. It is possible to find models in the literature to describe mechanical properties of amorphous polymers but most of them do not take into account the time parameter. In the same way, viscoelastic behaviour is often modelled by describing the solid as some combination of idealised elastic and viscous components such as a Hookean spring and a Newtonian dashpot. Among these compound models, the simplest are those of Maxwell, Kelvin-Voigt and Zener. Unfortunately these models are characterised by only one relaxation time¹⁻³.

By introducing fractional calculus tools in rheological models, it is possible to account for the distribution of relaxation times associated with amorphous polymer response. This approach has been used successfully over the past few years in the case of molten polymers⁴⁻⁶.

We shall extend this approach to viscoelastic behaviour modelling of glassy amorphous polymers in the temperature range from $T_g - 190^\circ\text{C}$ to $T_g + 25^\circ\text{C}$. These kinds of polymers are affected by the structural recovery phenomenon or physical ageing (at least between about $T_g - 90^\circ\text{C}$ and T_g ⁷), which has an influence on viscoelastic properties such as deformation aptitude, dynamic modulus etc.⁸.

In this paper, we try to quantify the effect of the structural recovery phenomenon on the viscoelastic behaviour of amorphous polymers and particularly on the parameters of our fractional calculus model.

Fractional calculus model

This fractional calculus model is based on the following

idea: the constitutive equation associated with the response of a perfect elastic material is the well known Hook's law:

$$\sigma(t) = \tau^0 E D_t^0 \varepsilon(t) = E \varepsilon(t) \quad (1)$$



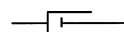
where:

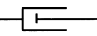


is a spring element, $\sigma(t)$ is the applied stress, E is the elastic modulus, $D_t^0 \varepsilon(t)$ is the differentiation of zero order of the strain with respect to time.

The constitutive equation associated with the response of a perfect viscous material is the well-known Newton's law:

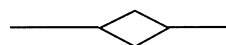
$$\sigma(t) = \tau^1 E D_t^1 \varepsilon(t) = \eta \frac{d\varepsilon(t)}{dt} \quad (2)$$

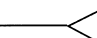


where  is a dashpot element, $\tau^1 = \eta/E$ is the relaxation time of the dashpot element, $D_t^1 \varepsilon(t)$ is the differentiation of first order of the strain with respect to time and η is the viscosity.

Now in the same way, if we have a viscoelastic material, its response can be represented by the following constitutive equation⁹:

$$\sigma(t) = \tau^\alpha E D_t^\alpha \varepsilon(t) \quad (3)$$



where  is a springpot element, $D_t^\alpha \varepsilon(t)$ is the fractional derivative of α order of the strain with respect to time with evidently $0 \leq \alpha \leq 1$.

According to the definition of the fractional derivative of

* To whom correspondence should be addressed

α order, equation (3) can be rewritten as¹⁰:

$$\sigma(t) = E\tau^\alpha \frac{1}{\Gamma(1-\alpha)} \frac{d}{dt} \left(\int_0^t (t-y)^{-\alpha} \varepsilon(y) dy \right) \quad (4)$$

where $\Gamma(\alpha)$ is the Gamma function:

$$\Gamma(\alpha) = \int_0^\infty (e^{-u} u^{\alpha-1}) du, \text{ with } \alpha > 0 \quad (5)$$

The classical linear solid model or Zener model is obtained by adding a second spring in parallel with a Maxwell unit (Figure 1).

For a sinusoidal loading where:

$$\varepsilon^* = \varepsilon_0 e^{i\omega t}, \sigma^* = \sigma_0 e^{i(\omega t + \delta)}, \sigma^* = E^* \varepsilon^* \quad (6)$$

where ω is the angular frequency and $E^* = E' + iE''$ is the complex modulus. E' and E'' the real and imaginary parts of the dynamic modulus are defined in Zener model by:

$$E' = E_0 + \frac{(E_\infty - E_0)\omega^2\tau^2}{1 + \omega^2\tau^2} \quad (7)$$

$$E'' = \frac{(E_\infty - E_0)\omega\tau}{1 + \omega^2\tau^2} \quad (8)$$

This model does not represent real viscoelastic behaviour of amorphous polymers, for example, the Cole-Cole diagram for the Zener model is symmetrical (Figure 2), but the real viscoelastic response for amorphous polymers is asymmetrical^{11,12}, which is due to the inequality of the viscoelastic behaviour response over a long time and a short time.

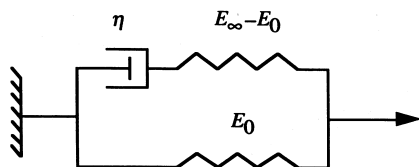


Figure 1 The Zener solid model

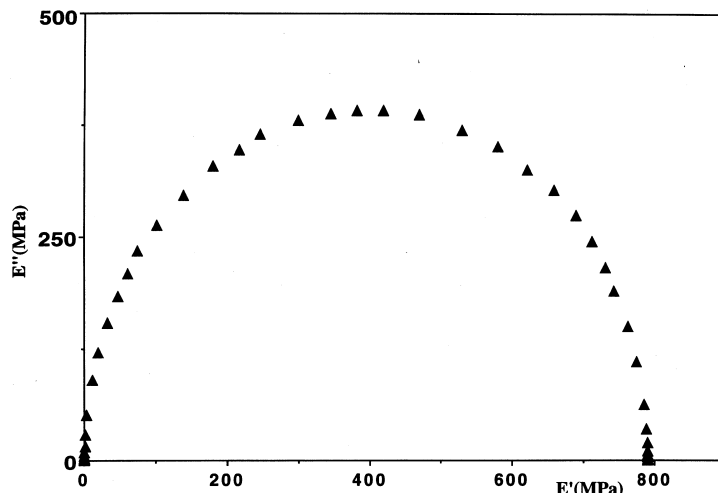


Figure 2 Cole-Cole diagram for the Zener solid model

Fractional Zener model (FZM)

In viscoelasticity, the Zener model, is often used as a first approximation for the study of the viscoelastic solids. If the dashpot is replaced by a springpot (Figure 3) then the Zener model becomes a fractional Zener model¹³ (FZM).

The stress-strain relationship for this model is¹⁴:

$$\sigma + \tau^\alpha D_t^\alpha \sigma = E_\infty \tau^\alpha D_t^\alpha \varepsilon(t) + E_0 \varepsilon(t) \text{ with } 0 \leq \alpha < 1 \quad (10)$$

For a sinusoidal loading, we have:

$$E' = E_0 \frac{(1+k)(\omega\tau)^{2\alpha} + (\omega\tau)^\alpha (2+k) \cos\left(\alpha \frac{\pi}{2}\right) + 1}{\left[1 + (\omega\tau)^\alpha \cos\left(\alpha \frac{\pi}{2}\right)\right]^2 + \left[(\omega\tau)^\alpha \sin\left(\alpha \frac{\pi}{2}\right)\right]^2} \quad (11)$$

and

$$E'' = E_0 \frac{k(\omega\tau)^\alpha \sin\left(\alpha \frac{\pi}{2}\right)}{\left[1 + (\omega\tau)^\alpha \cos\left(\alpha \frac{\pi}{2}\right)\right]^2 + \left[(\omega\tau)^\alpha \sin\left(\alpha \frac{\pi}{2}\right)\right]^2} \quad (12)$$

where $k = (E_\infty - E_0)/E_0$, E_∞ is the unrelaxed modulus, E_0 is the relaxed modulus, ω is the angular frequency (rad/sec) with $\omega = 2\pi f$, f is the frequency (Hz).

The prediction of FZM (equation (11)) for the storage modulus E' versus frequency is plotted in Figure 4, for several values of α . The classical response for polymers can be obtained by choosing the values of α between 0 and 1. The respective Cole-Cole diagrams for the same values of α are shown in Figure 5. They are symmetrical independently of the value of α .

To obtain the classical asymmetric response for the Cole-Cole diagram in amorphous polymers we add a second springpot to FZM (Figure 6), where $D_t^\beta \varepsilon_2$ is the fractional derivative of β order of the ε_2 , with $0 < \beta \leq 1$, $D_t^\alpha \varepsilon_3$ is the fractional derivative of α order of the ε_3 , with $0 < \alpha \leq 1$, $\varepsilon_1, \varepsilon_4$ are the strains associated to the springs, $\varepsilon_2, \varepsilon_3$ are the strains associated to the springpots.

This model is characterised by three mechanisms. The first one, is associated with the viscoelastic behaviour at low temperature or at high frequency, the second one represents the viscoelastic behaviour at high temperature or at low frequency and the third one represents the elastic behaviour of the polymer.

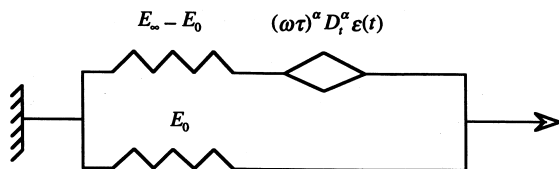
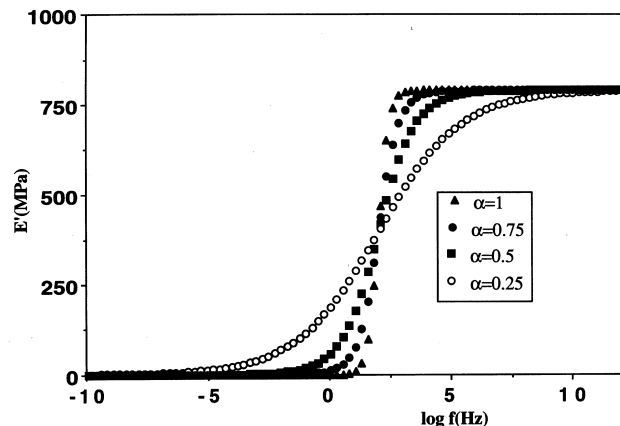


Figure 3 Fractional Zener model


 Figure 4 Storage modulus, E' , versus frequency for the fractional Zener model: (○) $\alpha = 0.25$; (■) $\alpha = 0.5$; (●) $\alpha = 0.75$; (▲) $\alpha = 1$

The dynamic modulus ($E^* = E' + iE''$), of this model can be calculated by using the Laplace and Fourier transforms:

$$E' = E_0 + \frac{(E_\infty - E_0)(1 + A_1)}{(1 + A_1)^2 + A_2^2} \quad (13)$$

$$E'' = \frac{(E_\infty - E_0)A_2}{(1 + A_1)^2 + A_2^2} \quad (14)$$

$$A_1 = \delta(\omega\tau)^{-b} \cos\left(b\frac{\pi}{2}\right) + (\omega\tau)^{-a} \cos\left(a\frac{\pi}{2}\right) \quad (15)$$

$$A_2 = \delta(\omega\tau)^{-b} \sin\left(b\frac{\pi}{2}\right) + (\omega\tau)^{-a} \sin\left(a\frac{\pi}{2}\right) \quad (16)$$

$$\tau = \tau_2 = \tau_1/s, \delta = s^{-b}, \alpha = -a, \beta = -b$$

with $0 < a \leq b \leq 1$.

Figure 7 shows the prediction of real modulus versus frequency for a constant value of α parameter (0.3) and different values of β parameter (0.3; 0.5; 0.8; 1). This prediction is consistent with the classical evolution of the real modulus with frequency. We can point out that:

- (1) at the lowest frequencies, the curves exhibit positive slopes which depend on β parameter. This means that effectively the β springpot is mainly associated with the viscoelastic behaviour at low frequency or high temperature.
- (2) at the highest frequencies, the curves are superimposed. This means that the α parameter (constant in this case) is associated with the viscoelastic behaviour at high frequency or low temperature.
- (3) between these two regions, and with decreasing frequency, a steep decrease in E' is noticeable and the slope can be changed by varying α and β . This region corresponds to the anelastic manifestation of the glass transition.

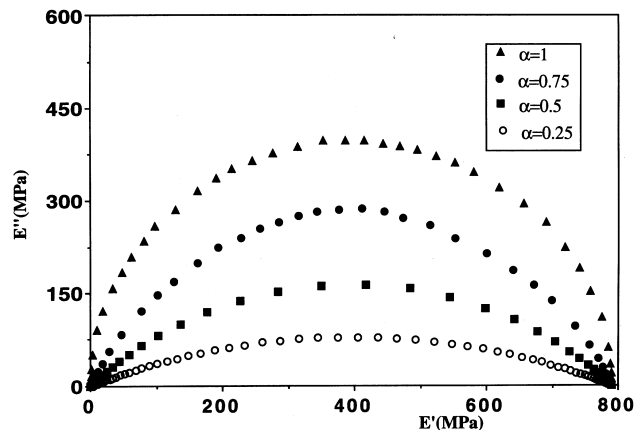
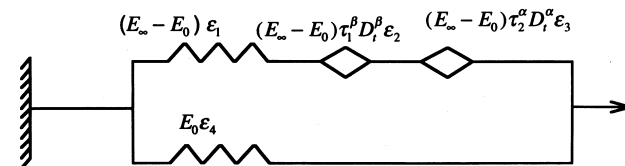

 Figure 5 Cole-Cole diagram for the fractional Zener model: (○) $\alpha = 0.25$; (■) $\alpha = 0.5$; (●) $\alpha = 0.75$; (▲) $\alpha = 1$


Figure 6 Fractional Zener model with two spring-pots

The Cole-Cole diagram for this model (equations (13) and (14)) is shown in Figure 8. We obtain on the one hand the classical asymmetric diagrams and on the other hand the same behaviour of the α and β parameters concerning the response of the model at high or low frequency/temperature. The real viscoelastic response of amorphous polymers can be predicted by our model and the comparison between theory and experimental data over a wide range of frequency can be established by using dynamic mechanical measurements.

EXPERIMENTAL

Material

Samples of poly(methyl methacrylate) PMMA were obtained from ELF, France who prepared and characterised it. Its molecular weight is 3×10^6 (g/mol) and its polydispersity index is 2.3.

Dynamic mechanical measurements

Dynamic mechanical measurements were performed by using a DMTA MKIII (Rheometric Scientific) operating in double cantilever bending mode.

This instrument provided the real (E') and the imaginary (E'') parts of the dynamic modulus (E^*) as a function of the temperature (under isochronal conditions) or of the frequency (under isothermal conditions).

In this work, isothermal dynamic data were obtained at intervals of 5°C from 60 to 160°C at different frequencies: 0.1; 1; 3; 5; 10 and 20 Hz.

Rectangular samples ($35 \times 6 \times 2$ mm³) were used. Before the DMTA run sample was dried for 1 h under vacuum at 80°C , it was next kept for 1 h at 130°C ($T_g + 20^\circ\text{C}$) always under vacuum in order to erase thermo-mechanical history and any water effect.

RESULTS AND DISCUSSION

According to the frequency-temperature superimposition principle¹⁵, the curves of E' versus frequency, in the glass

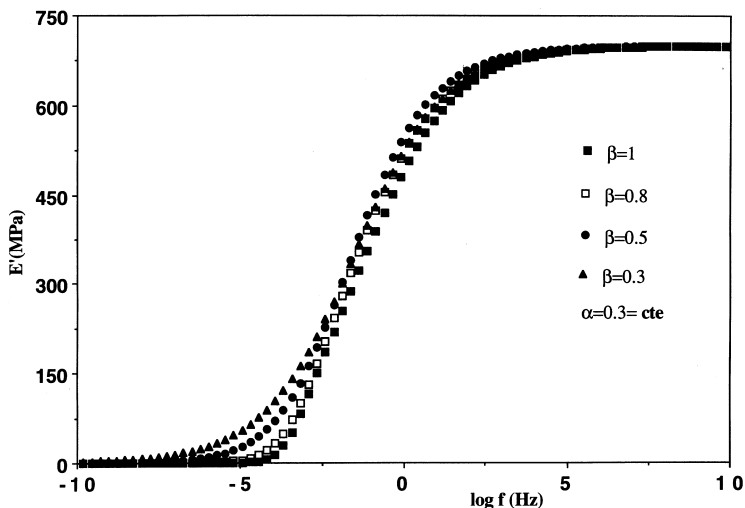


Figure 7 Storage modulus, E' , versus frequency for the fractional Zener model with two spring-pots: $\alpha = 0.3 = \text{cte}$; (\blacktriangle) $\beta = 0.3$; (\bullet) $\beta = 0.5$; (\square) $\beta = 0.8$; (\blacksquare) $\beta = 1$

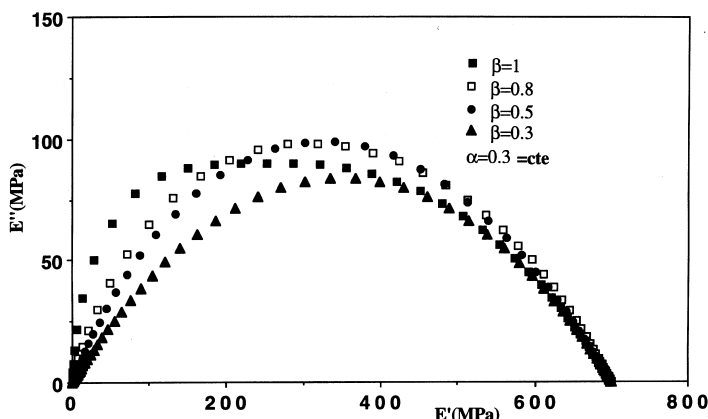


Figure 8 The Cole-Cole diagram for the fractional Zener model with two spring-pots: $\alpha = 0.3 = \text{cte}$; (\blacktriangle) $\beta = 0.3$; (\bullet) $\beta = 0.5$; (\square) $\beta = 0.8$; (\blacksquare) $\beta = 1$

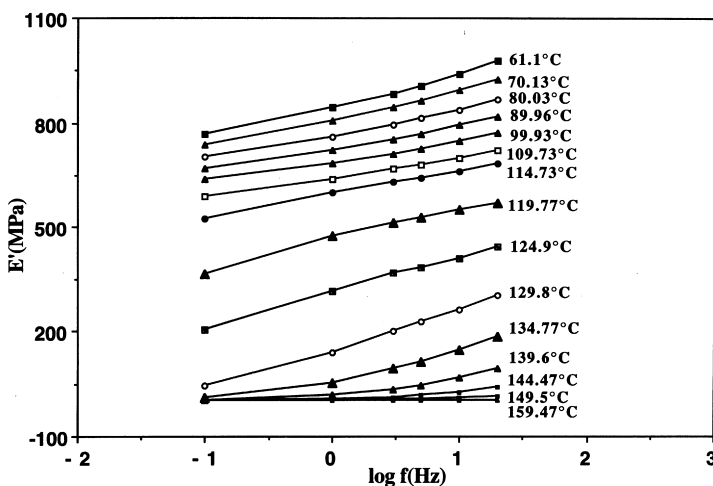


Figure 9 PMMA storage modulus, E' , versus frequency over the 60–160°C temperature range

transition region, can be reduced to a unique master curve at a reference temperature, provided it has the appropriate horizontal shift along the frequency scale. Figure 9 shows some isothermal modulus curves measured at temperatures between 60 and 160°C in the frequency range of 0.1 to 20 Hz. A master curve of dynamic modulus against logarithm of the frequency was generated by shifting each

curve horizontally on to the curve at the chosen reference temperature (Table 1).

Reference temperature used for PMMA was 109.73°C, the master plot obtained over a wide range frequency is given in Figure 10.

From this experimental master curve, we can obtain the unrelaxed modulus, E_∞ , and the relaxed modulus E_0 which

will subsequently be used in equations (13) and (14). $\tau_1 = 200$ s and $\tau_2 = 600$ s are the rheological parameters (Figure 6) and are constant for a given reference temperature.

Figure 11 shows the good agreement between the model ($\alpha = 0.33$ and $\beta = 0.79$) and the master curve displayed in Figure 10.

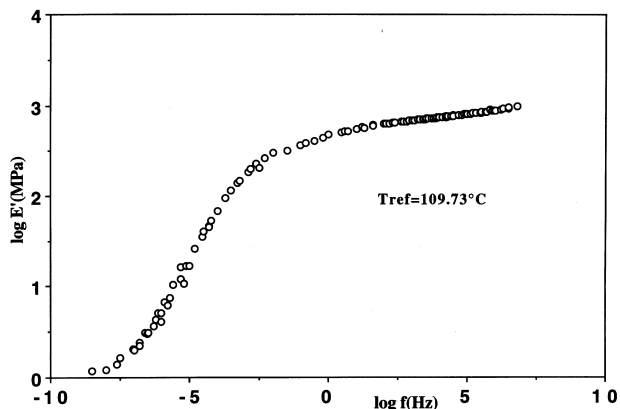


Figure 10 Master curve for the PMMA sample (obtained from Fig. 9)

Table 1 Shift factors required to obtain the experimental master curve displayed in Figure 10

Temperature (°C)	$\log(a_T)$
61.1	5.2
65.16	5
70.13	4.5
75.17	4
80.03	3.5
85.03	3
89.96	2.5
95	2
99.93	1.5
104.86	1
109.73	0
114.73	-0.8
119.77	-1.6
124.9	-2.5
129.8	-3.7
134.77	-4.5
139.6	-5.3

Concerning E'' values, Figure 12 displays the experimental Cole–Cole diagram and the diagram obtained from our model with the same values of α and β parameters (0.33 and 0.79, respectively). We observe very good agreement for temperatures higher than 111.5°C ($\approx T_g$), but a limit of the model is observed below this temperature. This low temperature experimental behaviour is associated with the existence of secondary relaxation. In the case of PMMA there is a relaxation at about 60°C ^{7,16,17} and β relaxation at about room temperature¹⁸.

The properties of PMMA and particularly viscoelastic properties will be affected by these phenomena as well as by the structural relaxation or physical ageing in this range of temperature.

Several authors, have proposed models in order to describe the viscoelastic behaviour of amorphous polymers near T_g , such models have been extensively described and applied elsewhere to amorphous and semicrystalline polymers^{19,20}.

By using the fractional calculus method, we attempted to extend the modelling to the behaviour of PMMA not only over a wide range of frequency but over a wide range of temperature too and to take account of the physical ageing phenomenon.

In this way, we will try firstly to characterise the effect of physical ageing in the shape of a Cole–Cole diagram, secondly to obtain experimentally the Cole–Cole diagram of PMMA between $T_g - 190^\circ\text{C}$ and $T_g + 25^\circ\text{C}$ and finally to propose an extended viscoelastic model.

In the following, we present experimental results obtained by DMTA in isothermal aged samples.

Effect of physical ageing on viscoelastic properties of PMMA

PMMA ageing has been studied by DMTA in isochronal scans at a frequency of 1 Hz and a heating rate of $1^\circ\text{C}/\text{min}$. The storage modulus, E' , and damping factor, $\tan \delta$, have been measured between 30 and 130°C .

The thermal cycle used to obtain a reference PMMA sample is the same as previously described.

After the first DMTA run, of the reference sample until 130°C , without removing the sample, it was cooled down to the ageing temperature 90°C and kept at this temperature for a time of 20 h. Next, the sample was cooled to room temperature in an ambient atmosphere and the second

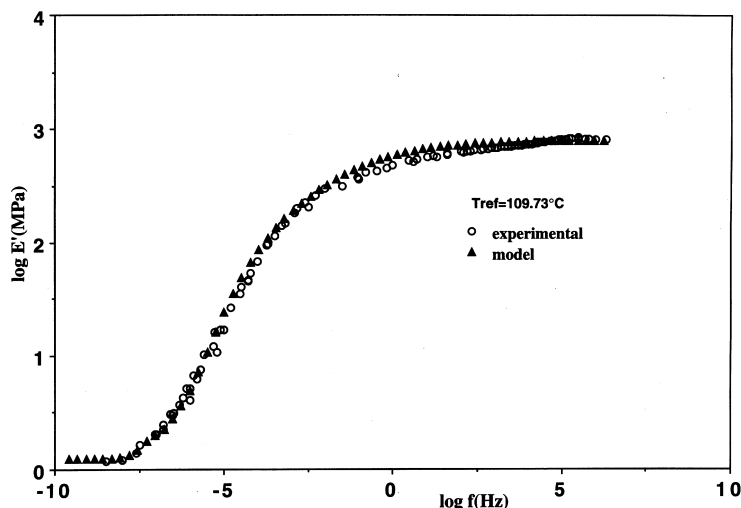


Figure 11 PMMA storage modulus, E' , (obtained from Fig. 10): (O) experimental data; (▲) prediction of FZM (Eq. 13)

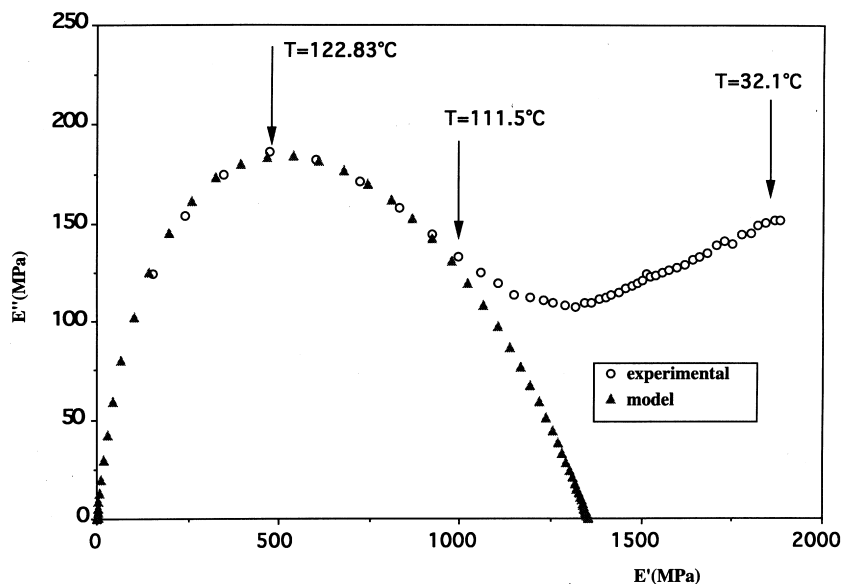


Figure 12 Comparison between the experimental PMMA Cole-Cole diagram and the corresponding calculated model FZM (Equations (13) and (14)): (○) experimental data; (▲) model

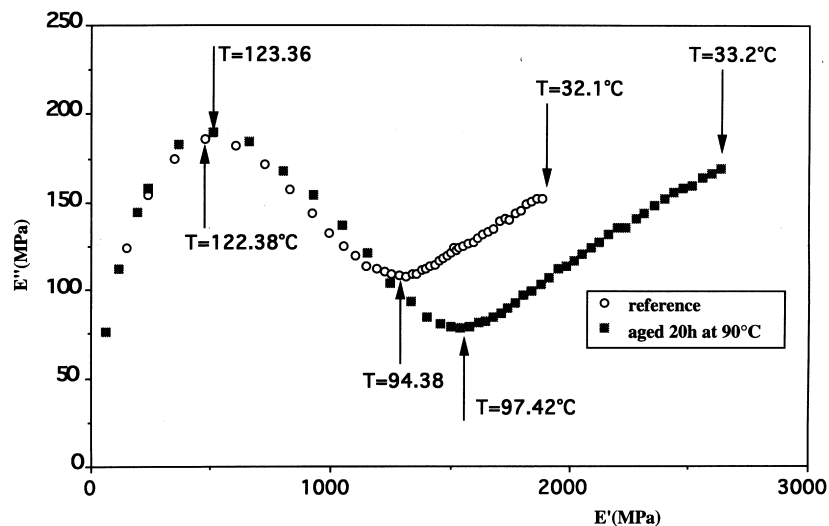


Figure 13 Comparison in the complex plane between reference and aged samples for PMMA: (○) reference sample; (■) aged sample

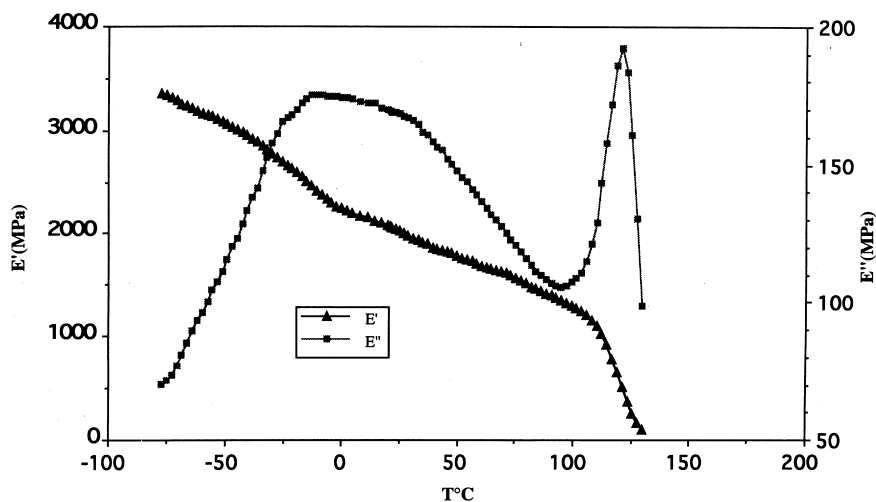


Figure 14 Viscoelastic characteristics versus temperature at 1 Hz for the PMMA reference sample: (▲) storage modulus, E' ; (■) loss modulus, E''

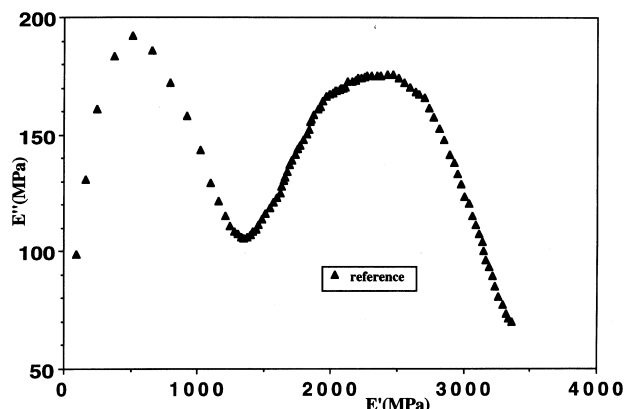


Figure 15 The Cole–Cole diagram for the PMMA reference sample at 1 Hz over a wide range of temperature (obtained from Fig. 14).

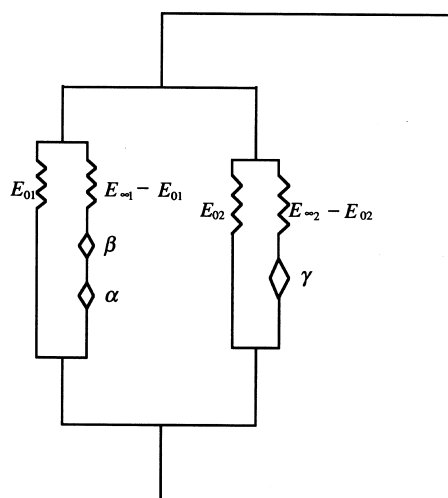


Figure 16 Extended fractional solid (EFS) model

DMTA run was recorded under the same experimental conditions. The Cole–Cole diagrams of reference and aged samples are displayed in Figure 13.

We note that in the high temperature zone, the slopes of the Cole–Cole diagrams are the same. This behaviour is consistent with the fact that physical ageing is not observed in this zone, because amorphous polymers are considered in thermodynamic equilibrium at temperatures well above the glass transition temperature²¹. The difference between Cole–Cole diagrams begin after the E'' maximum ($T_{\alpha} \approx 122^{\circ}\text{C}$) and they increase for lower temperatures.

Concerning the slopes in Cole–Cole diagrams, related in our case to the fractional parameters α and β (Figure 8) and used in the literature (biparabolic model)¹⁹ as molecular mobility parameters, our results show clearly that not only the existence of secondary relaxations but also structural recovery, or physical ageing, must be taken into account in the lower temperature domain. Experimental extrapolation in this case can be delicate.

Before we propose the extended viscoelastic model a sample of reference PMMA was characterised by DMTA under isochronal conditions (1 Hz) between -75°C ($\approx T_g - 190^{\circ}\text{C}$) to 140°C ($\approx T_g + 25^{\circ}\text{C}$) and a heating rate of $1^{\circ}\text{C}/\text{min}$ (Figure 14).

Figure 14 shows two relaxation modes: a very broad secondary relaxation mode β at around -10°C and the primary relaxation mode α , associated to the anelastic

manifestation of the PMMA glass transition, at around 120°C . These experimental DMTA spectra allowed us to obtain the experimental Cole–Cole diagrams displayed in Figure 15 and to propose the extended fractional solid (EFS) model to describe the viscoelastic behaviour of PMMA over a wide range of temperature (Figure 16). It is composed of two fractional models which are combined in parallel: the first one, characterised by α and β parameters, associated with the viscoelastic behaviour of amorphous polymers around the glass transition region and the second one, characterised by the γ parameter, associated with the viscoelastic behaviour in the low temperature region.

The real and imaginary parts of the dynamic modulus obtained by using our EFS model are:

$$E' = E_{01} + \frac{(E_{\infty 1} - E_{01})(1 + B_1)}{(1 + B_1)^2 + B_2^2} + E_{02} \frac{(1 + k)(\omega\tau_3)^{2\gamma} + (\omega\tau_3)^{\gamma}(2 + k) \cos\left(\gamma\frac{\pi}{2}\right)}{\left[1 + (\omega\tau_3)^{\gamma} \cos\left(\gamma\frac{\pi}{2}\right)\right]^2 + \left[(\omega\tau_3)^{\gamma} \sin\left(\gamma\frac{\pi}{2}\right)\right]^2}$$

$$E'' = \frac{(E_{\infty 1} - E_{01})B_2}{(1 + B_1)^2 + B_2^2} + E_{02} \frac{k(\omega\tau)^{\gamma} \sin\left(\gamma\frac{\pi}{2}\right)}{\left[1 + (\omega\tau_3)^{\gamma} \cos\left(\gamma\frac{\pi}{2}\right)\right]^2 + \left[(\omega\tau_3)^{\gamma} \sin\left(\gamma\frac{\pi}{2}\right)\right]^2}$$

where

$$B_1 = D(\omega\tau)^{-\beta} \cos\left(\beta\frac{\pi}{2}\right) + (\omega\tau)^{-\alpha} \cos\left(\alpha\frac{\pi}{2}\right)$$

$$B_2 = -\left[D(\omega\tau)^{-\beta} \sin\left(\beta\frac{\pi}{2}\right) + (\omega\tau)^{-\alpha} \sin\left(\alpha\frac{\pi}{2}\right)\right]$$

$$D = \left(\frac{\tau_1}{\tau_2}\right)^{-\beta}$$

$$k = \frac{E_{\infty 2} - E_{02}}{E_{02}} \text{ with } 0 < \gamma \leq \alpha \leq \beta \leq 1.$$

Figure 17 shows the Cole–Cole diagram predicted by our EFS model in three different cases:

- (1) for a constant value of α and γ parameters and different values of β parameter (Figure 17a), the variation of β parameter affects mainly the high temperature zone (temperatures higher than the glass transition temperature).
- (2) for a constant value of β and γ parameters and different values of α parameter (Figure 17b), the neighbourhood of the first maximum corresponding to the anelastic manifestation of the glass transition is mainly affected.
- (3) for a constant value of α and β parameters and different values of γ parameter (Figure 17c), the second peak associated with secondary relaxation is mainly affected.

Physical ageing affects mainly the region between the two maxima so the α and γ parameters must be related to structural recovery.

In order to evaluate the ability of our EFS model to predict the evolution of the dynamic complex modulus over a wide temperature range we show the excellent agreement between the prediction of the model (with $\alpha = 0.32$, $\beta = 0.79$ and $\gamma = 0.195$) and the experimental data of the reference PMMA sample in Figure 18.

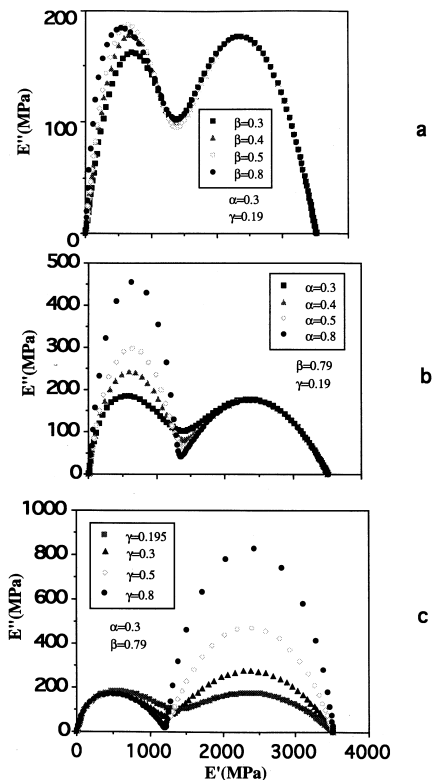


Figure 17 Predictions of the EFS model in the complex plane for: (a) $\alpha = 0.3 = \text{cte}$, $\gamma = 0.19 = \text{cte}$, (■) $\beta = 0.3$, (▲) $\beta = 0.4$, (○) $\beta = 0.5$, (●) $\beta = 0.8$; (b) $\beta = 0.79 = \text{cte}$, $\gamma = 0.19 = \text{cte}$, (■) $\alpha = 0.3$, (▲) $\alpha = 0.4$, (○) $\alpha = 0.5$, (●) $\alpha = 0.8$; (c) $\alpha = 0.3 = \text{cte}$, $\beta = 0.79 = \text{cte}$, (■) $\gamma = 0.195$, (▲) $\gamma = 0.3$, (○) $\gamma = 0.5$, (●) $\gamma = 0.8$

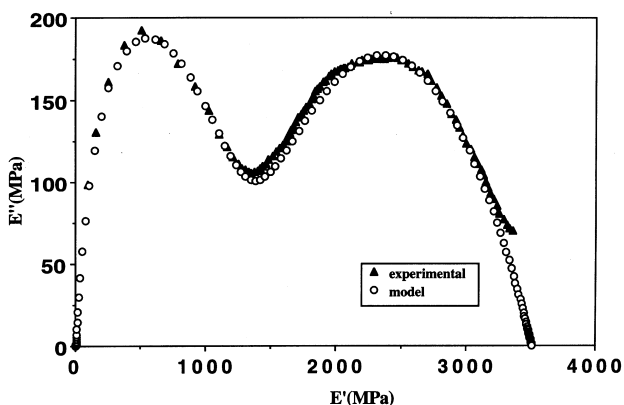


Figure 18 Comparison in the complex plane between the experimental PMMA data at 1 Hz and the EFS model: (▲) experimental data; (○) model

The α and γ parameters describe the evolution of viscoelastic behaviour of amorphous polymers from the lower temperature to the glass transition temperature region and they may be associated with the distribution of relaxation times $H(\tau)$ which are directly related to the molecular mobility of amorphous polymers. The α and β parameters can be evaluated from the thermal history of the polymer and they would be dependent on the temperature and the time of physical ageing.

So, physical ageing has been characterised by using DMTA and the following thermal cycle:

- (1) annealing the sample at a temperature well above the glass transition ($T_g + 20^\circ\text{C}$) in order to erase the thermal history of the material. Annealing was carried out for 1 h at 130°C .

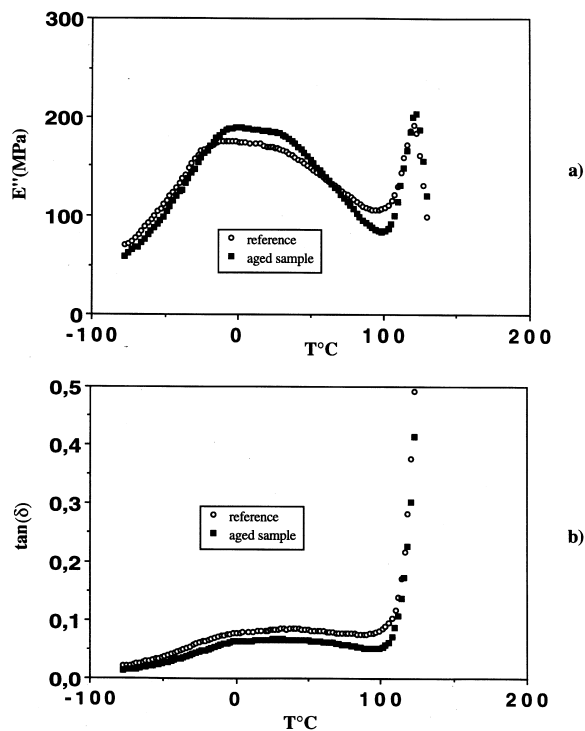


Figure 19 (a) Loss modulus, E'' , versus temperature at 1 Hz for the reference (○) and the aged (■) PMMA samples. (b) Loss factor, $\tan \delta$, versus temperature at 1 Hz for the reference (○) and the aged (■) PMMA samples

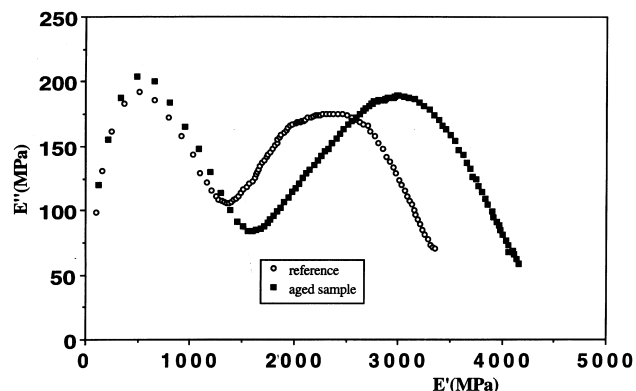


Figure 20 Comparison in the complex plane between the reference and the aged PMMA samples: (○) reference sample; (■) aged sample

- (2) cooling the sample down to the ageing temperature (90°C) and keeping the sample at this temperature for 20 h.
- (3) cooling the sample to -80°C in a nitrogen atmosphere and recording the DMTA thermogram with a heating rate of $1^\circ\text{C}/\text{min}$ at 1 Hz.

DMTA spectra (E'' and $\tan \delta$ versus temperature) of the reference and aged sample are shown in Figure 19, the corresponding Cole–Cole diagrams are displayed in Figure 20.

The agreement obtained between our fractional rheological and experimental data of the aged sample was average to good (Figure 21). We summarise in Table 2 the effect of physical ageing on our parameters.

In the temperature region above T_g we observe that the viscoelastic behaviour of the aged sample is unaffected by physical ageing, so the β parameter is not a function of ageing time.

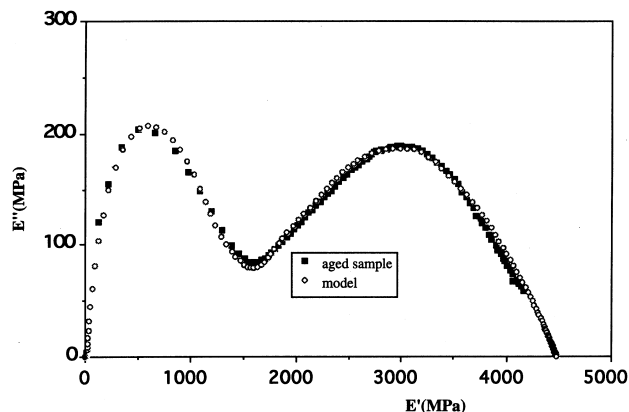


Figure 21 Comparison in the complex plane between the aged experimental PMMA sample at 1 Hz and the EFS model: (■) aged sample; (○) model

Table 2 Effect of physical ageing on our model parameters

Parameters of EFS model	Reference sample	Aged sample
α	0.32	0.304
β	0.79	0.79
γ	0.195	0.15

On the contrary, as expected, the region concerning α and γ parameters is in fact clearly correlated with physical ageing. The α parameter varies slightly but the value of the γ parameter is strongly affected by this structural recovery phenomenon.

The objective of our study was to show the coherence of the fractional derivative approach over a wide range of frequency and temperature (from $T_g - 190^\circ\text{C}$ to $T_g + 25^\circ\text{C}$).

We underline that this method allows one to calculate the analytical theoretical equations of the real and imaginary parts of the dynamic modulus and it is possible to have analytical access to the relaxation time spectra $H(\tau)$.

We are conscious that the model parameters are phenomenological parameters, and they are not physically meaningful and future studies should concentrate on their molecular origin.

Systematic studies of the physical ageing phenomenon are in progress so as to have a relation between the model parameters and the time and temperature of physical ageing and the effect of this phenomenon on the time relaxation spectrum $H(\tau)$.

CONCLUSION

The fractional calculus approach gives predictions of the entire viscoelastic behaviour of the amorphous polymers in

the glassy zone and it allows us to obtain the analytical equations for all viscoelastic functions.

The biparabolic model represents the viscoelastic behaviour of amorphous polymers between the transition and rubber zones and it has a limit in the glassy zone because of the secondary relaxation and the structural recovery of this type of polymer.

The physical ageing phenomenon affects the viscoelastic property of amorphous polymers in the glassy state between the glassy transition zone and the secondary relaxation zone, and only the α and γ parameters are affected by this phenomenon.

ACKNOWLEDGEMENTS

One of the authors (M. Alcoutlabi) wishes to thank the Aga-Khan Foundation for their generous support during the period of this study. The authors thank Dr. David Brown for stimulating discussions and for critically reading an earlier version of the manuscript.

REFERENCES

- Ferry, J. D., *Viscoelastic Behavior of Polymers*, 3rd edn. J. Wiley and Sons, New York, 1980.
- Tschoegl, N. W., *The Phenomenological Theory of Linear Viscoelastic Behavior, An Introduction*. Springer-Verlag, New York, 1988.
- Ward, I. M., *Mechanical Properties of Solid Polymers*. J. Wiley and Sons, New York, 1990.
- Baumgaertel, M., Schausberger, A. and Winter, H. H., *Rheol. Acta*, 1990, **29**, 400.
- Friedrich, C., Braun, H. and Weese, J., *Polym. Engng Sci.*, 1995, **35**, 1661.
- Palade, L. I., Verney, V. and Attané, P., *Rheol. Acta*, 1996, **35**, 265.
- Martinez-Vega, J. J., PhD thesis, University of Poitiers, France, 1986.
- Struik, L. C. E., *Physical Ageing in Amorphous Polymers and Other Materials*. Elsevier, Amsterdam, 1978.
- Stiassnie, M., *Appl. Math. Modelling*, 1979, **3**, 300.
- Bagly, R. L. and Torvik, P. J., *J. Rheol.*, 1983, **27**, 201.
- Huet, C., Thesis, University of Paris, France, 1963.
- Chauchard, J. and Jeanne, P., *Annales des Composites*, 1987, **2**, 103.
- Koeller, R. C., *J. Appl. Mechanics*, 1984, **51**, 299.
- Bagly, R. L. and Torvik, P. J., *J. Rheol.*, 1986, **30**, 133.
- Williams, M. L., and Landel, R. F. and Ferry, J. D., *J. Am. Chem. Soc.*, 1955, 3701.
- Gacougnolle, J. L., Martinez-Vega, J. J. and Lacabanne, C., Paper presented at 9th International Conference on Deformation Yield and Fracture of Polymers, UK, 11–14 April 1994.
- Martinez-Vega, J. J., Diffalah, M., Lacabanne, C. and Gacougnolle, J. L., Paper presented at 9th International Conference on Deformation Yield and Fracture of Polymers, UK, 11–14 April 1994.
- Muzeau, E., *PhD thesis*, INSA, Lyon, France, 1992.
- Perez, J., *Physique et Mécanique des Polymères Amorphes*. Lavoisier, Paris, 1992.
- Alberola, N., Cavaille, J. Y. and Perez, J., *Eur. Polymer J.*, 1992, **28**, 949.
- Kovacs, A. J., Stratton, D. A. and Ferry, J. D., *J. Phys. Chem.*, 1963, **67**, 152.